SUPPLEMENT MATERIAL

Detailed Methods

Animal model. Male mice, overexpressing PPARα in the heart, driven by the alpha myosin heavy chain promoter, (MHC-PPARα) and non-transgenic, littermates (NTG) weighing ~25g at 12 weeks of age were used for this study (1). Mice were backcrossed to C57Bl/6J six times before this study was conducted. Prior to the protocols, mice received either a regular chow diet (RCD) or a high fat diet (HFD, Teklad #97268) for two weeks. The Teklad #97268 is a formulation that provides 43% of calories from fat. The source of the fat is corn oil and beef tallow. The calculated fatty acid content is as follows: 3g/kg 14:0, 35.0 g/kg 16:0, 21.8 g/kg 18:0, 60.6 g/kg 18:1, 54.2 g/kg 18:2, 1.5 g/kg 18:3. Measured levels of circulating TAG and non-esterified fatty acids in NTG and MHC-PPARα mice, in support of a previously published study, were not different between NTG and MHC-PPARα mice either during a RCD or HFD (1). Mice had free access to food and water while being housed under controlled temperature and lighting. All experimental procedures were approved by the University of Illinois at Chicago Animal Care and Use Committee.

Isolated heart protocols. 12-week old animals were heparinized (50 U/10 g, i.p.) and anesthetized with ketamine (80 mg/kg, i.p.) plus xylazine (12 mg/kg, i.p.). Hearts were excised and retrogradely perfused (60 mm Hg) with modified Krebs-Henseleit buffer (118.5 mM NaCl, 4.7 mM KCl, 1.5 mM $CaCl_2$, 1.2 mM $MgSO_4$ and 1.2 mM KH_2PO_4) equilibrated with 95% O_2/5% CO_2, at 37°C, and containing 0.4 mM unlabeled palmitate/ fatty acid free albumin complex (3:1 molar ratio) and 10 mM glucose. A water-filled latex balloon was fitted into the left ventricle and set to a diastolic pressure of 5 mmHg. Left ventricular developed pressure (LVDP) and heart rate (HR) were continuously recorded with a pressure transducer and digital recording system (Powerlab, AD Instruments, Colorado Springs, CO). Rate-pressure product (RPP) was calculated as the product of heart rate and developed pressure. Temperature was maintained at 37^{o}C.

Oxygen consumption was determined with a blood gas analyzer (GEM Premier 300, Instrumentation Laboratory) and calculated as oxygen uptake (volume percent from A-V difference) multiplied by mean coronary blood flow (mL/min).

For TAG dynamics, isolated hearts from both NTG and MHC-PPARα mice were perfused in a 14.1 T NMR magnet at baseline workload (NTG N=7; MHC-PPARα N= 12) or with adrenergic challenge (0.1 micromole isoproterenol) (NTG N=5; MHC-PPARα N= 6). At the start of each protocol, the hearts continued to be supplied buffer containing unlabeled palmitate/albumin complex and glucose for 10 minutes to ensure metabolic equilibrium and allow for collection of ^{13}C-NMR background signals of naturally abundant ^{13}C (1.1%). Isotopic enrichment was initiated by switching the perfusate supply to ^{13}C-enriched buffer containing 0.4 mM [2,4,6,8,10,12,14,16 - $^{13}C_8$] palmitate (Isotec, Inc., Miamisburg, OH) plus 10 mM unlabeled glucose.

Perfusion with ^{13}C-enriched media continued for 20 minutes at baseline workload for mice on a regular chow diet (RCD) (MHC-PPARα n=10; NTG n=12), from mice on a high fat diet (HFD) (Teklad #97268) (MHC-PPARα n = 7; NTG, n = 4), and for 10 minutes with adrenergic challenge (0.1 μM isoproterenol) (MHC-PPARα n=5; NTG n=8). Additional hearts were perfused for 120 minutes to ensure stability of TAG turnover and content over time (n=4). At the end of each protocol, hearts were frozen in liquid N_2 cooled tongs.

For determination of palmitate oxidation rates, hearts from MHC-PPARα and NTG mice on a RCD (MHC-PPARα , n = 6; NTG, n = 4) and on a HFD (MHC-PPARα n = 7; NTG, n = 5) were perfused for 30 minutes with 0.4 mM or 1.2 mM [4,6,8,10,12,14,16,-$^{13}C_7$] palmitate and 10 mM glucose. [4,6,8,10,12,14,16,-$^{13}C_7$] palmitate was used for ease of analysis for the C4 carbon of glutamate in the ^{13}C-NMR spectra due to overlapping resonances from the C4 position of glutamate and C2 position of

acyl intermediates. Sequential ^{13}C-NMR spectra were collected and hearts were frozen in liquid N_2 cooled tongs for biochemical analysis (2-3).

NMR spectroscopy and tissue chemistry. Measurements of TAG turnover were performed on intact beating hearts that were situated within a 10 mm broad band NMR probe inside a 14.1 T NMR magnet. Sequential, proton-decoupled ^{13}C NMR spectra were acquired (2 min each) with natural ^{13}C abundance correction using previously reported NMR methods (4-5). Magnetic field homogeneity was optimized by shimming to a proton line width of 10-20 Hz.

Carbon-13 enrichment of TAG in the intact heart was monitored from the NMR signal at 30.5 ppm from the TAG methylene groups and TAG turnover was calculated from total TAG content and enrichment over time (6-8). Kinetic analysis of dynamic ^{13}C-spectra from intact, beating hearts was performed as previously reported from our laboratory (4-5, 7-8). Carbon spectra were acquired at 100 MHz, with bilevel broad-band decoupling and subtracted from naturally abundant endogenous ^{13}C signal.

Tissue metabolites were extracted from frozen heart tissue using 7% perchloric acid and neutralized with KOH. Tissue extracts were analyzed spectrophotometrically and flurometically for quantificaiton (9-10). Glutamate concentration was determined with glutamate dehydrogenase and diaphorase (Roche L-Glutamic acid colorimetric kit.) α-Ketoglutarate content was measured by coupling glutamate-oxaloacetate transaminate (GOT, Roche) with malate dehydrogenase (MDH, Roche) in the presence of excess L-aspartate. Aspartate concentration was measured by coupling GOT with MDH similar to α-ketoglutarate with the exception of excess α-ketoglutarate. Citrate content was determined with citrate lyase (Roche) and MDH. *In vitro* high-resolution ^{13}C NMR spectra of tissue extracts reconstituted I 0.5 mL of D_2O were collected with a 5 mm ^{13}C probe (Bruker Instruments, Billerica, MA). Analysis was performed to determine fractional enrichment of [2-^{13}C] acetyl CoA (11-12).

Lipid extracts were obtained from heart samples and triacylglycerides (TAG) quantified by colorimetric assay, as previously described (Wako Pure Chemical Industries.) (2, 5, 13). TAG was isolated, saponified, and the fractional ^{13}C enrichment of the fatty acids assessed by liquid chromatography/mass-spectrometry (LC/MS) analysis (Waters X-terra C18MS column; MS:scan m/z 100-600 Fragmentor 75V Negative ESI). LCFA content in TAG, of carbon lengths 12-18, were determined by LCMS and are reported as a percentage of total LCFA present.

TAG turnover and ^{13}C enrichment dynamics Total TAG turnover (nanomoles TAG/min/mg protein) was quantified from measured ^{13}C enrichment rates and the endpoint ^{13}C enrichment of TAG over the time course of the experiment, as previously described (5-8). Linear analysis of TAG turnover was calculated as TAG content multiplied by the ^{13}C fractional enrichment of TAG /enrichment duration. Under steady state conditions the rate of TAG synthesis equals degradation.

Rates of palmitate unit turnover within the TAG pool were determined from TAG turnover rates and the percentage of acyl units represented by palmitate ([^{12}C + ^{13}C] palmitate) present in the TAG pool. LCMS analysis enabled determination of the percentage of each LCFA present in the TAG pool. From the stoichiometry of 3 long chain fatty acyl groups per TAG molecule and the percentage of palmitate present in the TAG pool, TAG turnover rates were converted to rates of palmitate unit turnover within the TAG pool.

Kinetic Analysis Oxidative Rates. A set of nine differential equations describes the concentration history of the ^{13}C in each metabolite and developed in our laboratory was modified to include the additional, rate-determining components of long chain fatty acid uptake into the mitochondria. With a single 9x1 vector q to represent the fractional enrichment of each compartment as a function of time, the model is described in matrix form as

$$\frac{d}{dt}q = M_{TCA} \cdot q + U_{Acetyl-CoA}$$

where M_{TCA} is a 9x9 matrix characteristic of the TCA cycle, its elements are determined by the TCA cycle flux (V_{TCA}), the interconversion rates between the TCA cycle intermediate and glutamate or aspartate (F_1 and F_2), the level of anaplerosis (y), and the concentrations of each metabolite. The input vector, $U_{Acetyl\text{-}CoA}$, is governed by the fraction of ^{13}C enriched acetyl-CoAentering the TCA cycle through citrate synthase (F_c). The only non-zero element in $U_{Acetyl\text{-}CoA}$ corresponds to the labeling of the 4-carbon position of citrate since [2-^{13}C] acetyl-CoA enters the TCA cycle through citrate synthase to enrich the 4-carbon position of citrate (3, 14-15). The nine differential equation in series are:

$$\frac{d}{dt}CIT4 = \frac{V_{TCA}}{[CIT]} \cdot (F_c - CIT4)$$

$$\frac{d}{dt}\alpha KG4 = \frac{V_{TCA}}{[\alpha KG]} \cdot CIT4 - \frac{V_{TCA} + F_1}{[\alpha KG]} \cdot \alpha KG4 + \frac{F_1}{[\alpha KG]} \cdot GLU4$$

$$\frac{d}{dt}GLU4 = \frac{F_1}{[GLU]} \cdot (\alpha KG4 - GLU4)$$

$$\frac{d}{dt}CIT2 = \frac{V_{TCA}}{[CIT]} \cdot (OAA2 - CIT2)$$

$$\frac{d}{dt}\alpha KG2 = \frac{V_{TCA}}{[\alpha KG]} \cdot CIT2 - \frac{V_{TCA} + F_1}{[\alpha KG]} \cdot \alpha KG2 + \frac{F_1}{[\alpha KG]} \cdot GLU2$$

$$\frac{d}{dt}GLU2 = \frac{F_1}{[GLU]} \cdot (\alpha KG2 - GLU2)$$

$$\frac{d}{dt}MAL2 = \frac{V_{TCA}}{[MAL]} \cdot [\frac{1}{2} \cdot \alpha KG2 + \frac{1}{2} \cdot \alpha KG4 - (1 + y) \cdot MAL2]$$

$$\frac{d}{dt}OAA2 = \frac{V_{TCA}}{[OAA]} \cdot MAL2 - \frac{V_{TCA} + F_2}{[OAA]} \cdot OAA2 + \frac{F_2}{[OAA]} \cdot ASP2$$

$$\frac{d}{dt}ASP2 = \frac{F_2}{[ASP]} \cdot (OAA2 - ASP2)$$

Where CIT, aKG, GLU, MAL, OAA, and ASP denote the metabolites citrate, a-ketoglutarate, glutamate, malate, oxaloacetate, and aspartate, respectively, with the corresponding number of the ^{13}C enriched carbon position indicated. Where CIT4 is the fractional enrichment level of ^{13}C at the 4-carbon position of citrate; (i.e., CIT4=[(4-^{13}C)CIT]/[CIT]). The equation describing malate enrichment includes anaplerotic and cataplerotic effects (4, 11, 14-15). F_1 and F_2 are fluxes for interconversion via both transamination and membrane transport, between a-ketoglutarate and glutamate, and between aspartate and oxaloacetate, respectively. Under the current experimental conditions of limited aspartate and alanine, $F_1 = F_2$ (3, 11, 14-15).

A penalty function was applied, using MVO_2 as an external measured parameter, to constrain optimization of fitting data to the kinetic model within the known physiological limits (11, 14):

$$\tilde{f}(\mathbf{p}) = \sum_{i=1}^{m} \left(\frac{d(t_i, \mathbf{p}) - s(t_i)}{\sigma_i} \right)^2 + \left(\frac{V_{TCA} - V_{MVO_2}}{\sigma_{MVO_2}} \right)^2$$

Where t_i are the data-sampling times, $d(t_i,p)$ are glutamate enrichment predicted by the model, $s(t_i)$ are the NMR measurements of glutamate enrichment, and σ_i are the error associate with NMR measurements. V_{TCA} and V_{MVO2} are measured from oxygen consumption rate and σ_{MVO2} is the error associate with the measurement of oxygen consumption (11, 14).

The rate of palmitate oxidation (R) was calculated, under these precise experimental and isotopic enrichment conditions, as the product of V_{TCA} and acetyl CoA enrichment from ^{13}C palmitate (F_c) divided by 8 to account for the 8 acetyl groups produced from the 16 carbon palmitate (V_{TCA} x F_c/8).

RNA extraction and quantitative RT-PCR. Total RNA was extracted from hearts with Trizol reagent (Invitrogen Corporation, Carlsbad, CA) and 3 µg of RNA were reverse transcribed using Superscript III Reverse Transcriptase (Invitrogen) (16). The resulting cDNA were subjected to quantitative real-time RT-PCR on an ABI Prism 7900HT instrument (Applied Biosystems, Foster City, CA) in 384-well plate format using SYBR Green as a probe and a ROX internal reference dye (Invitrogen). Primers were selected from PrimerBank or designed using Primer3Plus and the appropriate GenBank reference sequence (17-18). Gene names, primer sequences, and product sizes are presented in Supplementary Table S1. All reactions were performed in triplicate. Relative quantification was performed by interpolating crossing point data on an independent standard curve. Product size was confirmed by agarose gel electrophoresis and ethidium bromide staining. Data were corrected for loading by expressing them relative to the levels of the invariant transcript Ppia (NM_018874) and normalized to wild-type controls on standard chow (a.u. = 1.0).

Statistical Analysis Inter-group statistics were analyzed using one-way ANOVA analysis with the Tukey post-test. Statistical significance was established at 5% probability ($P < 0.05$). All reported values are reported as averages ± SEM.

References

1. Finck BN, Han X, Courtois M, Aimond F, Nerbonne JM, Kovacs A, Gross RW, Kelly DP. A critical role for PPARα-mediated lipotoxicity in the pathogenesis of diabetic cardiomyopathy: modulation by dietary fat content. *PNAS*, 2003;100;1226-31.
2. Lopaschuk GD, Hansen CA, and Neely JR. Fatty acid metabolism in hearts containing elevated levels of coenzyme A. *Am J Physiol* 250: H351-H359, 1986.
3. Lewandowski ED, Doumen C, White LT, LaNoue KF, Damico LA, Yu X. Multiplet structure of 13C NMR signal from glutamate and direct detection of TCA cycle intermediates. *Magn Reson Med*. 1996;35:149-154.
4. O'Donnell, JM, Alpert, NM, White, LT, Lewandowski, ED. Coupling of mitochondrial fatty acid uptake to oxidative flux in the intact heart. *Biophysical J*. 2002;82:11-18.
5. O'Donnell JM, Zampino M, Alpert NM, Fasano MJ, Geenen DL, Lewandowski ED. Accelerated triacylglycerol turnover kinetics in hearts of diabetic rats include evidence for compartmented lipid storage. *Amer J Physiol Endocrinol Metab*. 2006; 290: E448-E455.
6. Schaffer JE. Lipotoxicity: when tissues overeat *Curr. Opin. Lipidol.* 2003;14:281-7.17. O'Donnell, J. M., Fields, A. D., Sorokina, N., Lewandowski, E. D. (2008) *J. Mol. Cell. Cariol.* 44, 315-22
7. O'Donnell JM, Fields AD, Sorokina N, Lewandowski ED. Absence of endogenous lipid oxidation in heart failure exposes limitations for triacylglycerol storage and turnover. *J Mol Cell Cardiol*. 2008;44:315-22.
8. Lehman JJ, Boudina S, Banke NH, Sambandam N, Han X, Young DM, Leone TC, Gross RW, Lewandowski ED, Abel ED, Kelly DP. The transcriptional coactivator PGC-1α is essential for maximal and efficient cardiac mitochondrial fatty acid oxidation and lipid homeostasis. *Am. J. Physiol. Heart Circ. Physiol.*, 2008;295:H185-96
9. Bowyer DE, and King JP. Methods for the rapid separation and estimation of the major lipids of arteries and other tissues by thin-layer chromatography on small plates followed by microchemical assays. *J Chromatog* 143: 473-490, 1977.
10. Williamson JR, Corkey BE. Assays of intermediates of the citric acid cycle and related compounds by fluorometric enzyme methods. In: Colowick SP, Kaplan NO, eds. *Methods in Enzymology*. New York, NY: editors. Academic; 1969: 439-513..
11. Yu X, White LT, Doumen C, Daminco LA, LaNoue KF, Alpert NM, Lewandowski ED Kinetic analysis of dynamic ^{13}C NMR spectra: metabolic flux, regulation, and compartmentation in hearts. *Biophys. J.* 1995;69:2090-102.
12. Malloy CR, Sherry AD, Jeffrey FMH. Evaluation of carbon flux and substrate selection through alternate pathways involving the citric acid cycle of the heart by 13C NMR spectroscopy. *J Biol Chem.* 1988;265:6964-6971.
13. Atkinson LL, Kozak R, Kelly SE, Onay-Besikci A, Russell JC, and Lopaschuk GD. Potential mechanisms and consequences of cardiac TAG accumulation in insulin-resistant rats. *Am J Physiol Endocrinol Metab* 284: E923-E930, 2003.
14. Yu X, Alpert NM, and Lewandowski ED. Modeling enrichment kinetics from dynamic ^{13}C NMR spectra: theoretical analysis and practical considerations. *Am. J. Physiol. (Cell Physiol. 41)*1997; 272: C2037-C2048.
15. O'Donnell JM, NM Alpert, White LT, ED Lewandowski. Coupling of Mitochondrial Fatty Acid Uptake to Oxidative Flux in the Intact Heart. *Biophys J* 2008;2:11-18.
16. Sena S, Rasmussen IR, Wende AR, McQueen AP, Theobald HA, Wilde N, Pereira RO, Litwin SE, Berger JP, Abel ED. Cardiac hypertrophy caused by peroxisome proliferator-activated receptor-g agonist treatment occurs independently of changes in myocardial insulin signaling. *Endocrinology*. 2007;148:6047-6053.

17. Spandidos A, Wang X, Wang H, Dragnev S, Thurber T, Seed B. A comprehensive collection of experimentally validated primers for Polymerase Chain Reaction quantitation of murine transcript abundance. *BMC Genomics.* 2008;9:633.
18. Untergasser A, Nijveen H, Rao X, Bisseling T, Geurts R, Leunissen JA. Primer3Plus, an enhanced web interface to Primer3. *Nucleic Acids Res.* 2007;35(Web Server issue):W71-74.

Online Supplemental Data

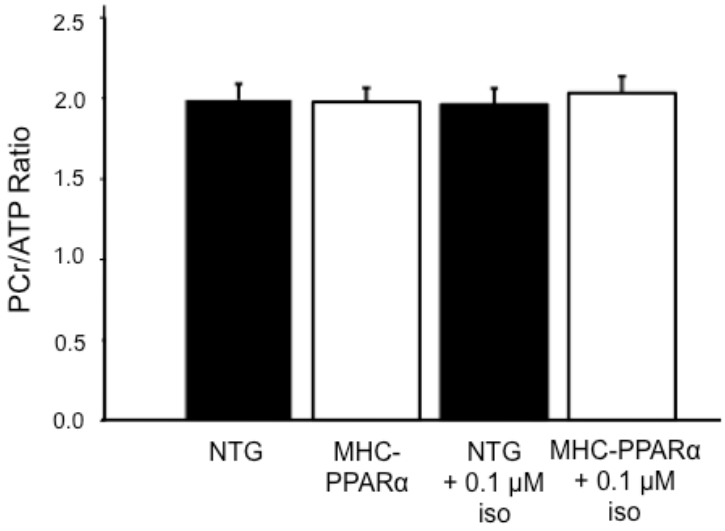

Online Figure I. Ratio of intracellular PCr to ATP in NTG and MHC-PPARα hearts at baseline and during adrenergic stimulation (NTG: N=10; MHC-PPARα: N=9; NTG + iso: N=8; MHC-PPARα + iso: N=7). There were no significant differences between NTG and MHC-PPARα hearts at baseline or during β-adrenergic stimulation. PCr and ATP are measured by ^{31}P NMR at 0ppm and 16 ppm, respectively.

Gene Symbol	Gene Name	Ref Seq #	Primer Blank ID	Sequence (5'-3') Fwd top; Rev bottom	Product Size (bp)
Agpat3	1-acylglycerol-3 phosphate O-acyltransferase 3	NM_053014	27229278a1	CTGCTTGCCTACCT GAAGACC GATACGGCGGTAT AGGTGCTT	141
Agpat5	1-acylglycerolphospha te acyltransferase-epsilon	NM_026792	27229077a1	CACACGTACTCTA TGCGCTAC AAGAAGAGCACCA TGTTCTGG	173
Cel	Carboxyl ester lipase	BC006872	6753406a3	ACAACACCTATGG GCAAGAAG CTCCTCCCCGTCAT ACAGGTA	173
Dgat1	Diacylglyerol Acetyltransferase 1	NM_010046	n/a	TGGCTGCATTTCA GATTGAG ACAGGTTGACATC CCGGTAG	216
Dgat2	Diacylglyerol Acetyltransferase 2	NM_026384	n/a	TCTCAGCCCTCCA AGACATC GCCAGCCAGGTGA AGTAGAG	192
Dgke	Diacylglycerol kinase, epsilon	NM_019505	9506541a1	TGGTCCTATGGAC GCTGTG CTGAACAGGTCGG TGTCACG	142
Gpam	Glycerol-3-phosphate acyltransferase, mitochondrial	NM_008149	6680057a1	ACAGTTGGCACAA TAGACGTTT CCTTCCATTTCAGT GTTGCAGA	139
Lpin1	Lipin 1 isoform b; fatty liver dystrophy	NM_015763	27923941a1	CATGCTTCGGAAA GTCCTTCA GGTTATTCTTTGGC GTCAACCT	100
MgII	Monoglyceride lipase	AK006949	12840263a1	ACCATGCTGTGAT GCTCTCTG CAAACGCCTCGGG GATAACC	100
Mttp	Microsomal triglyceride transfer protein	NM_008642	667896a1	CTCTTGGCAGTGC TTTTTCTCT GAGCTTGTATAGC CGCTCATT	102
Ppap2c	Phosphatidic acid phosphate type 2c	BC010332	12838015a1	CTCACGGTCCGCT ATGTTTCA GGTCAGCGTCAGT GACAGAC	105
Ppara	Peroxisome proliferative	NM_001113 418	n/a	GAGAATCCACGAA GCCTACC	172

	activated receptor, alpha			AATCGGACCTCTG CCTCTTT	
Ppia	Peptidylprolyl isomerase; Cyclophilin	NM_008907	n/a	AGCACTGGAGAGA AAGGATTGG TCTTCTTGCTGGTC TTGCCATT	349
Pnliprp1	Pancreatic lipase related protein 1	NM_018874	9256628a3	GCAGAACTGGGTG GTTGACAT CGTGTAGGTAGTC TGAGAGCCT	100

Online Table I. Gene and sequence information for expression studies.